Biochemical and Biophysical Research Communications 463 (2015) 262–267

Contents lists available at ScienceDirect

Biochemical and Biophysical Research Communications

journal homepage: www.elsevier.com/locate/ybbrc

Palmitate promotes autophagy and apoptosis through ROS-dependent JNK and p38 MAPK

Jing Liu [a], Fen Chang [a], Fang Li [a], Hui Fu [a], Jinlan Wang [a], Shangli Zhang [a], Jing Zhao [a, **], Deling Yin [b, *]

[a] Institute of Developmental Biology, School of Life Science, Shandong University, Jinan 250100, China
[b] Department of Internal Medicine, College of Medicine, East Tennessee State University, Johnson City, TN 37614, USA

ARTICLE INFO

Article history:
Received 22 April 2015
Available online 19 May 2015

Keywords:
Palmitate
Apoptosis
Autophagy
ROS
JNK
p38 MAPK

ABSTRACT

Palmitate (PA), one of the most prevalent saturated fatty acids, causes myocardial dysfunction. However, the mechanisms by which PA induces cell apoptosis and autophagy remain to be elucidated. We showed that autophagy was induced in an mTORC1-dependent way and played a protective role against PA-induced apoptosis, which was verified by pretreatment with 3-methyladenine (3MA) and rapamycin. However, p62 began to accumulate after 18 h treatment with PA, suggesting prolonged exposure to PA lead to an impairment of autophagic flux. PA enhanced ROS production as well as activated p38-mitogen-activated protein kinase (p38 MAPK) and c-jun NH_2 terminal kinases (JNKs). The antioxidant N-Acety-L-Cysteine (NAC) was found to attenuate the JNK and p38 MAPK activation with a concomitant reduction of PA-induced autophagy and apoptosis. Furthermore, both JNK and p38 MAPK inhibitors were shown to directly abrogate caspase 7 cleavage as well as the conversion of LC3BI to LC3BII. Thus, we demonstrate that PA stimulates autophagy and apoptosis via ROS-dependent JNK and p38 MAPK pathways.

1. Introduction

Excessive accumulation of lipid in cardiomyocytes has been suggested to play a direct and essential role in the progress of diabetes and other obesity associated cardiomyopathy. Non-esterified fatty acids (NEFAs), especially saturated fatty acids (SFAs), have been shown experimentally to induce myocardial dysfunction, among which PA is the most prevalent.

Reactive oxygen species (ROS) are mainly produced in mitochondria by normal cellular metabolism of oxygen and function as important molecules mediating normal physiological signaling [1]. However, overproduction of ROS inside cardiac cells triggered by environmental stress, such as ischemia or hypoxia, may cause serious damage to the cells. Finally, apoptosis will be initiated by ROS through both extrinsic and intrinsic pathways [2], which lead to cardiac remodeling and fibrosis. In addition, elevated ROS production followed by oxidative stress has been reported to induce autophagy in many disease states [3]. Several studies have proposed that PA promotes ROS production in different cardiac cell types [4–8]. Although Wei et al. reported that U0126, an inhibitor of extracellular signal-regulated kinase (ERK), reduces PA-induced apoptosis through partial suppression of intracellular ROS generation, there is no direct evidence to prove the involvement of ROS [4]. A recent study demonstrated that autophagy is induced by PA as an adaptive response to ER stress since it is sensitive to ER stress inhibition in H9c2 cells [9]. However, whether ROS plays a role in PA-induced autophagy and apoptosis remains unknown.

The mitogen-activated protein kinases (MAPKs) are activated in response to diverse stimuli and play a vital role in eukaryotic cells by regulating fundamental cellular processes, such as gene expression, cell proliferation, differentiation, migration, and apoptosis. ERK, JNK, and p38 constitute conventional MAPKs [10]. JNK, also described as the stress-activated protein kinases (SAPKs), is intensively activated by various stresses and functions via phosphorylating the NH2-terminus of the transcription factor c-Jun. In most cases, JNK has been reported to promote apoptosis, however, JNK activated by hypoxia-reoxygenation is suggested to play an anti-apoptotic role in neonatal cardiac myocytes [11]. P38 MAPK signaling has been shown to either promote apoptosis or enhance cell survival depending on the cell type and stimulus [12,13]. PA activates JNK and p38 MAPK in many cell types,

* Corresponding author.
** Corresponding author. Fax: +86 531 88565610.
E-mail addresses: jingzhao@sdu.edu.cn (J. Zhao), yin@etsu.edu (D. Yin).

http://dx.doi.org/10.1016/j.bbrc.2015.05.042
0006-291X/

including cardiomyocytes. However, the roles of JNK and p38 MAPK in PA-induced autophagy and apoptosis in H9c2 cells still remains unknown.

In the present study, we determined the relationship between ROS, JNK and p38 MAPK, focusing on their roles in the regulation of PA-induced autophagy and apoptosis in H9c2 cells.

2. Materials and methods

2.1. Reagents

Antibodies for caspase 3, caspase 7, Bcl2 and β-actin were purchased from Santa Cruz Biotechnology, Inc. Antibodies for LC3BII, phospho-JNK, phospho-p38 MAPK, JNK, p38 MAPK, phospho-p70S6K, p70S6K were obtained from Cell Signaling Technology. The antibody for p62 was obtained from Medical & Biological Laboratories Co., Ltd. The antibody for Bax was obtained from BBI Life Sciences Corporation. PA, SP600125, SB203580, rapamycin, Bafilomycin A1, chloroquine, 3-methyladenine, N-acetyl cysteine were purchased from Sigma–Aldrich. Fatty acid-free bovine serum albumin (BSA) was obtained from Sangon Bitotech.

2.2. PA–albumin complexes preparation

PA was conjugated with bovine serum albumin (BSA) before added to cell culture media according to a modified method described by Svedberg et al. [14]. Firstly, palmitic acid was dissolved in ethanol at 200 mmol/l and then diluted in 10% BSA to make final concentrations of 1–8 mmol/l. Fatty acid-free BSA containing low endotoxin was used. The pH of the stock solutions were adjusted to 7.4 before aseptic filteration. For individual experiments, H9c2 cells were treated with PA at final concentrations of 0.1–0.8 mmol/l by diluting stock solution (1:10) in 10% FBS–DMEM.

2.3. Cell culture

The embryonic rat heart tissue derived H9c2 cell line was obtained from the Chinese Academy of Sciences Cell Bank, Shanghai, China. H9c2 cells were cultured in Dulbecco's modified Eagle's medium (Gibco) supplemented with 10% (v/v) fetal bovine serum (Hyclone), 1% penicillin/streptomycin (v/v). The cells were cultured in a humidified atmosphere containing 5% CO_2 at 37 °C, and were subcultured when grown up to 90% confluency.

2.4. Apoptosis quantified by flow cytometry

Cell apoptosis was quantified using an AnnexinV-FITC/PI apoptosis kit (BioLegend) according to the manufacturer's instructions. After treatment, cells were collected and rinsed twice with cold PBS and then resuspended in 60 ul Annexin-binding buffer. The suspension was incubated with 100 ng/ml Annexin V-FITC for 30 min and then 2 μg/ml propidium iodide (PI) for 5 min in the dark at room temperature (RT). FITC or PI positive cells were determined using a flow cytometer (ImageStream^X MarkII, Amnis, USA). The fluorescence of FITC and PI were measured in the FL2 channel (488 nm) and FL4 channel (488 nm), respectively. The results were analyzed using IDEAS software (Amnis, USA).

2.5. Western blotting

Cells were harvested and washed twice with PBS and then lysed in RIPA buffer with protease and phosphatase inhibitors on ice for 10 min. The lysates were centrifugated at 12,000 rpm at 4 °C for 10 min. Equal amount of protein was loaded in each lane and separated by 12% (or 15%) SDS-polyacrylamide gel electrophoresis (PAGE). The separated proteins were transferred to PVDF membranes (Millipore, Bedford, MA), and then blocked in 5% non-fat milk for 1 h at RT. Membranes were probed with the appropriate primary antibodies overnight at 4 °C. After washing with TBST, the membrane were incubated with peroxidase-conjugated secondary antibody for 1 h at RT. Enhanced chemiluminescence reagent (Millipore, U.S.A) was used to detect the proteins, and the intensity of the bands was quantified by Image J software.

2.6. Intracellular ROS detection

Following PA treatment, intracellular ROS was detected by fluorescence microscope using dichlorofluorescein diacetate (DCFH-DA) staining. Briefly, the H9c2 cells were incubated with 5 μM DCFH-DA (Sigma–Aldrich) for 30 min at 37 °C in the dark, and were washed with serum-free medium for three times. The fluorescence was excited at the wavelength of 485 nm and the corresponding emission wavelength was 520 nm.

2.7. Statistical analysis

All data were presented as mean ± SEM. Student *t* test or one-way ANOVA analysis was performed using GraphPad Prism 5. *P* value <0.05 was considered to indicate a statistically significant difference.

3. Results

3.1. PA induces apoptosis in H9c2 cells

To examine the lipotoxic effects of PA on H9c2 cardiac cells, we treated H9c2 cells with PA at concentrations ranging from 0.1 to 0.8 mmol/l. Annexin V and propidium iodide (PI) staining followed by flow cytometry assay was used to test whether PA induces apoptosis. Results showed that PA effectively increased the Annexin V^+ and Annexin V^+/PI^+ cell population in a dose-dependent manner (Fig. 1A, B), suggesting that apoptosis was induced. When cells undergo apoptosis, executioner caspases (e.g., caspase3, caspse7) can be finally activated and in turn cleave other protein substrates within the cell. Poly (ADP-ribose) polymerase 1 (PARP-1) is one of the main targets of caspase 3. Both concluded in Bcl-2 family, Bcl-2 is anti-apoptotic, whereas Bax is pro-apoptotic. Therefore, we next examined the effects of PA on apoptosis related protein levels by Western blotting. As shown in Fig. 1C, PA triggered the cleavage of caspase 3, caspase 7 and PARP-1 in a dose-dependent manner. As the concentration of PA increased, Bcl-2 protein levels was gradually reduced and Bax elevated. These results indicate that PA induces caspase-dependent apoptotic cell death.

3.2. PA promotes mTORC1-dependent autophagy at an early stage, but blocks autophagic flux for prolonged treatment in H9c2 cells

To determine whether PA induced autophagy, we treated H9c2 cells with PA at various time-points. The conjugation of the soluble form of LC3 (LC3-I) with phosphatidylethanolamine and conversion to a nonsoluble form (LC3-II) has been generally recognized as a useful sign of autophagy; thus we examined the expression of LC3B-II. After treatment with PA (0.4 mmol/l) at various times, LC3B-II levels increased in a time-dependent manner (Fig. 2A). However, we couldn't ascertain whether the increase of LC3B-II levels was due to activation of autophagy or blockade of autophagy-lysosomes fusion. Thus we next measured protein levels of p62, a selective substrate of autophagy, for activation of the autophagic flux leads to p62 degradation. As Fig. 2A shows, a

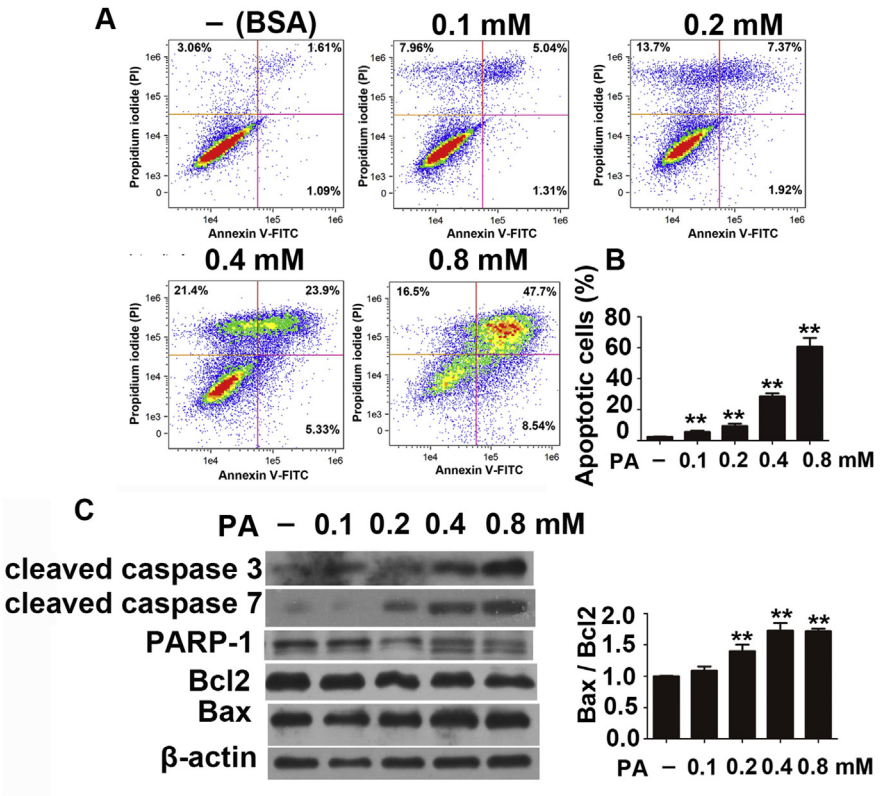

Fig. 1. PA induces apoptosis in H9c2 cells. (A) After treatment with increased doses of PA (0.1, 0.2, 0.4, 0.8 mM) for 12 h, induction of apoptosis in H9c2 cells was measured by Annexin-V/PI double-staining assay followed by flow cytometry analysis. BSA was added as a control. (B) The apoptotic proportion of H9c2 cells treated with PA was calculated according to the flow cytometry results. (C) Western blot analysis of apoptosis-related proteins expression after exposing to PA of different concentrations for 12 h. β-actin was probed as the loading control. Image J software was used to make quantitative analysis of Bcl-2 and Bax protein expressions by Western blot assay. The results are presented as mean ± SEM for at least three independent experiments. $^{**}p < 0.01$ vs. the control group (H9c2 cells treated with BSA).

marked decrease in p62 was detected as early as 3 h, then to a minimum at 6 h and 12 h. However, p62 was significantly elevated at 18 h and 24 h, indicating an impairment of autophagic flux. To further monitor autophagic fux induced by plmitate at the early stage, we co-treated H9c2 cells with both PA (0.4 mmol/l) and different autophagy inhibitors for 12 h. Fig. 2B demonstrated that LC3B-II protein levels was markedly attenuated in the presence of 3-methyladenine (3-MA), which could block the initiation of autophagy. Both Baflomycin A1 (Baf A1) and chloroquine (CQ) could disrupt the formation of autophagolysosomes via destroying the internal acidic environment of lysosome, and thereby leading to LC3II accumulation. Indeed, as shown in Fig. 2B, Baf A1and CQ markedly enhanced LC3BII protein levels in H9c2 cells treated with PA. Collectively, these data suggested that PA enhanced autophagic flux at the early stage (3 h–12 h), however, longer time exposue to PA leaded to impaired autophagic flux in H9c2 cells.

Consistent with the changes of autophagy marker proteins, the phosphorylation of p70S6K, a direct downstream target of mTORC1, was reduced from 6 h to 18 h, and then promoted to a higher level after PA treatment for 24 h (Fig. 2A), implying that the activity of mTORC1 was first suppressed when PA promoted autophagic flux for short-time treatment. However, mTORC1 was reactivated when the autophagic flux was blocked by prolonged PA treatment.

3.3. Autophagy protects H9c2 cells against PA-induced apoptosis

Since autophagy has dual roles in regulating cell survival and cell death, we next investigated the effect of PA-induced autophagy on apoptosis in H9c2 cells. We found that pretreatment with 3MA for 1 h followed by PA treatment for 12 h, greatly increased PA induced cleavage of caspase 3 (Fig. 2C). In contrast, rapamycin, a well-known autophagy inducer through targeting mTORC1, inhibited PA induced apoptosis (Fig. 2C). Taken together, autophagy may act as an adaptive way to protect H9c2 cells from PA-induced apoptosis. Prolonged treatment of PA impaired autophagic flux, and thereby turned cells to apoptotic pathways.

3.4. ROS mediate PA-induced autophagy and apoptosis of H9c2 cells

To investigate whether reactive oxygen species (ROS) play a role in the induction of apoptosis by PA, DCFH-DA, a fluorescent probe, was used to examine cellular ROS levels. As expected, H9c2 cells treated with PA showed a remarkable enhancement in fluorescence intensity compared to control group treated with BSA. H_2O_2 treated group was set as a positive control (Fig. 3A). N-acetyl-L-cysteine (NAC) is a usual anti-oxidant. Pre-incubation with NAC (0.5 mmol/l) markedly inhibited PA-induced ROS generation (Fig. 3A). We then tested the effect of NAC on apoptosis and autophagy. As shown in Fig. 3B, NAC inhibited PA induced apoptosis, and meanwhile, LC3BII protein levels was down-regulated. Taken together, PA induced overproduction of ROS, which contributed to autophagy and apoptosis of H9c2 cells.

3.5. PA induces autophagy and apoptosis in H9c2 cells through ROS-dependent JNK and p38 MAPK activation

Western blot analysis showed that both JNK and p38 MAPK were activated by PA in a dose-dependent manner (Fig. 4A).

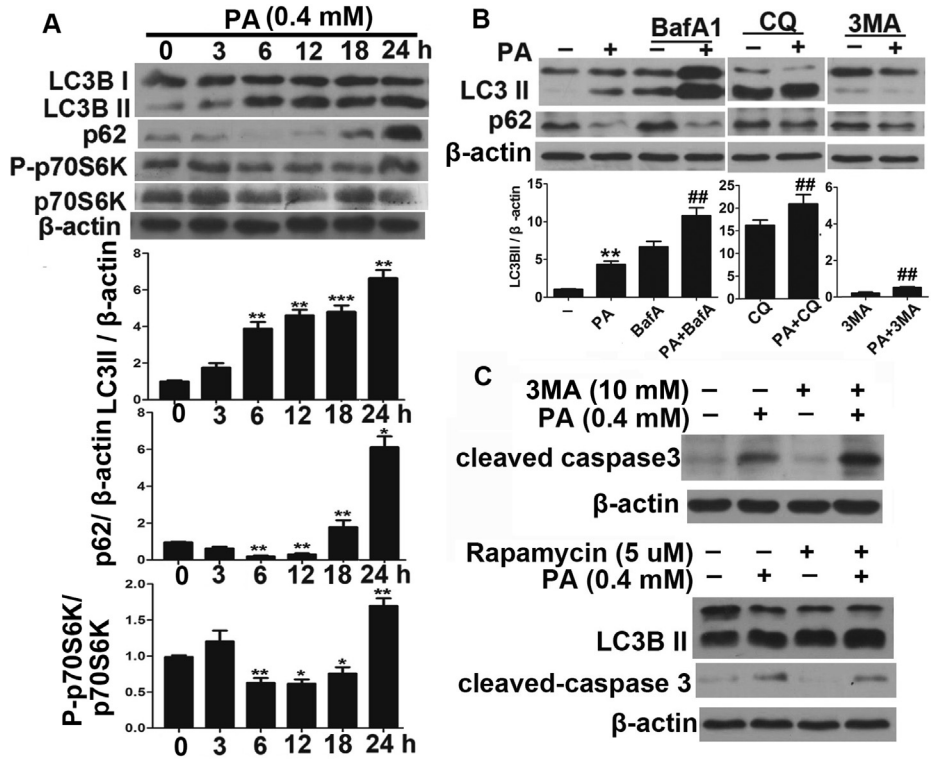

Fig. 2. PA induces protective autophagy against apoptosis in H9c2 cells. (A) Western blot analysis of autophagic markers after incubating H9c2 cells with 0.4 mM PA for indicated time points (3 h, 6 h, 12 h, 18 h, 24 h). Quantitative analysis of LC3BII, p62, p-p70S6K protein levels were made with Image J software. (B) LC3B II and p62 protein levels are determined by Western blot after pretreatment with autophagy inhibitors 3MA (10 mM), Bafilomycin A1 (60 nM) or chlorinated quinine (10 μM) respectively for 1 h followed by 0.4 mM PA for 12 h. (C) H9c2 cells were pretreated with 3MA or rapamycin to detect the effects of autophagy on apoptosis. β-actin is probed as loading control. Data represent the mean ± SEM of three independent experiments. $^{*}p < 0.05$, $^{**}p < 0.01$, $^{***}p < 0.001$ vs. BSA alone-treated group. ##$p < 0.01$, PA plus specific inhibitor-treated group versus PA alone-treated group.

Pretreated with either specific JNK inhibitor SP600125 or p38 MAPK inhibitor SB203580 directly inhibited PA-induced autophagy and apoptosis significantly (Fig. 4B). Since ROS have been reported to activate pro-apoptotic signaling pathways such as JNK, p38 MAPK via stimulation of upstream kinases, such as ASK1 [15], we use the antioxidant NAC to see whether PA-induced ROS lead to the activation of JNK and p38 MAPK. Expectedly, NAC obviously suppressed the phosphorylation of JNK and p38 MAPK (Fig. 4C). To sum up, ROS/JNK/p38 MAPK axis is involved in PA associated autophagy and apoptosis.

4. Discussion

Obesity and its associated conditions such as insulin resistance, dyslipidemia and hypertension, may contribute to multiple adverse effects on the heart, including cardiac hypertrophy, atherosclerosis, heart failure, and ischemic heart disease [16]. Cardiac lipotoxicity is closely associated with the progression of the above-mentioned diseases. However, the mechanisms by which overloaded fatty acids induce cardiac lipotoxicity are not completely known. Moreover, further studies are still necessary to investigate what mechanisms cardiomyocytes have developed to adapt to such lipotoxicity.

In our study, we report that PA (16:0), a long-chain saturated fatty acid, induces a remarkable cytotoxic effect on H9c2 cardiac cells. Both apoptosis and autophagy are induced by PA as previously reported. Although the pro-autophagic property of PA on H9c2 cells had been reported before, they limited to a short-time treatment. Here, we expanded the treatment for longer time and found that autophagic flux was damaged after 12 h. Short-time PA treatment promoted mTORC1-dependent autophagic flux and played a protective role against apoptosis. Further studies showed that ROS mediated PA-induced autophagy and apoptosis of H9c2 cells via activating JNK and p38 MAPK pathways.

Cardiac cell death, especially apoptosis, is a severe characteristic or consequence of obesity and its related pathologic heart conditions. Consistent with previous findings, data in Fig. 1A and B showed that PA treatment could obviously increase the apoptotic H9c2 cells. This was affirmed by increased cleavage of apoptosis-executive caspase 3 and caspase 7 and their main target, PARP-1. Moreover, PA treatment contributed to significantly increased Bax/Bcl-2 ratio (Fig. 1C) and obvious elevation of ROS shown in Fig. 3A, suggesting that mitochondrion-dependent intrinsic apoptosis pathways participate in PA associated lipotoxicity.

Whether autophagy is involved in cardiac metabolic stress or not depends on the state of metabolic syndrome. Cardiac autophagy was claimed to be suppressed, unaffected or disrupted in distinct obesity models *in vivo* [17–20]. In this study, Western blot analysis showed that from 3 h to 12 h, PA promoted the transformation from LC3BI to LC3BII and enhanced the degradation of p62, a specific autophagic substrate, implying the activation of autophagy. Co-treatment with 3MA for 12 h, suppressed PA-induced initiation of autophagy. Both BafA1 and CQ further enhanced the accumulation of LC3BII and p62. These data demonstrated a promotion of autophagic flux by PA. However, p62 began to accumulate while LC3BII levels remained high since 18 h, suggesting that continuous stimulation by PA for a relatively long time may lead to damage of autophagic flux and an aggravation of apoptosis. The mammalian target of rapamycin complex 1 (mTORC1) signal pathway is one classical mechanism in regulating

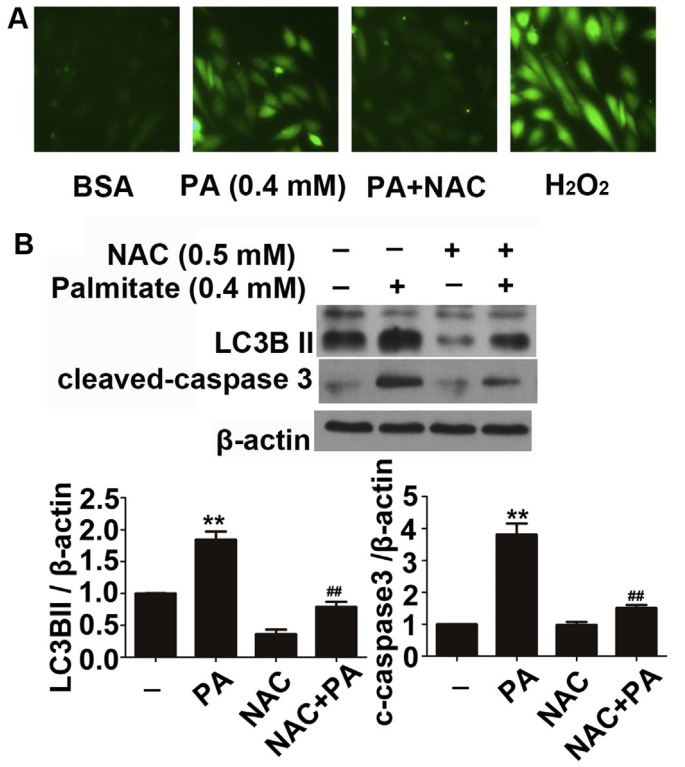

Fig. 3. ROS mediate PA-induced autophagy and apoptosis of H9c2 cells. (A) H9c2 cells were treated with 0.4 mM PA in the absence or presence of the antioxidant NAC (0.5 mM) or not for 12 h. Before end of treatment, cells were incubated with DCFH-DA and measured by a fluorescence microscope. Representative images (X 200) were presented to show ROS levels. (B) The effects of pre-incubation of NAC (0.5 mM) on protein levels of LC3B II, caspase 3 were detected by Western blot. Data represent the mean ± SEM of three independent experiments. $^{**}p < 0.01$, compared with BSA alone-treated group. ##p < 0.01, compared with PA alone-treated group.

autophagy. Activation of mTORC1 inhibits the initiation of autophagy through directly phosphorylating the ULK1-Atg13-FIP200 complex, which is essential for the formation of autophagosome [21,22]. Our data showed that the changes of phosphor-p70S6K, a direct downstream target of mTORC1, was in accordance with p62 levels. When autophagy was activated during 3 h–12 h, phosphor-p70S6K was inhibited, indicating that the activity of mTORC1 was suppressed. Consequently, these results supported that PA induced mTORC1-dependent autophagy for short-time treatment, however, autophagic flux may be blocked over time.

In normal physiological status, intracellular ROS are reduced by various antioxidant enzymes and are limited to very low levels. Environmental stress including lipotoxicity gives rise to ROS generation in different cell types, such as hepatocytes, pancreatic β-cells, adipocytes, HUVECs and myocardial cells we focused on right now [4,23–26]. Elevated ROS level is detrimental, which even ends up with cell death. Indeed, in agreement with the above description, our study showed that ROS levels were obviously enhanced in PA-treated H9c2 cells. Elimination of ROS with the anti-oxidant NAC significantly reduced ROS generation. A recent study demonstrated that deletion of macrophages JNK obviously inhibited obesity associated insulin resistance and inflammation, showing an important role of JNK in obesity [27]. Indeed, PA treatment in H9c2 cells activated JNK and p38 MAPK in a dose-dependent manner in our study. We next investigated whether ROS was involved in PA-induced apoptosis and autophagy. As expected, pretreatment with NAC notably abolished PA-induced apoptosis, evidenced by decreased caspase 3 cleavage. Meanwhile, NAC obviously reduced expression of the autophagic marker LC3BII as well as suppressed the activation of JNK and p38 MAPK triggered by PA. These data suggested that ROS play a vital role in PA induced apoptosis and autophagy. We should note that our results are in contrast with what had been previously observed in neonatal rat ventricular myocytes [8,28]. In neonatal rat ventricular myocytes, NAC and MAPK inhibitors failed to rescue PA-induced apoptosis. However,

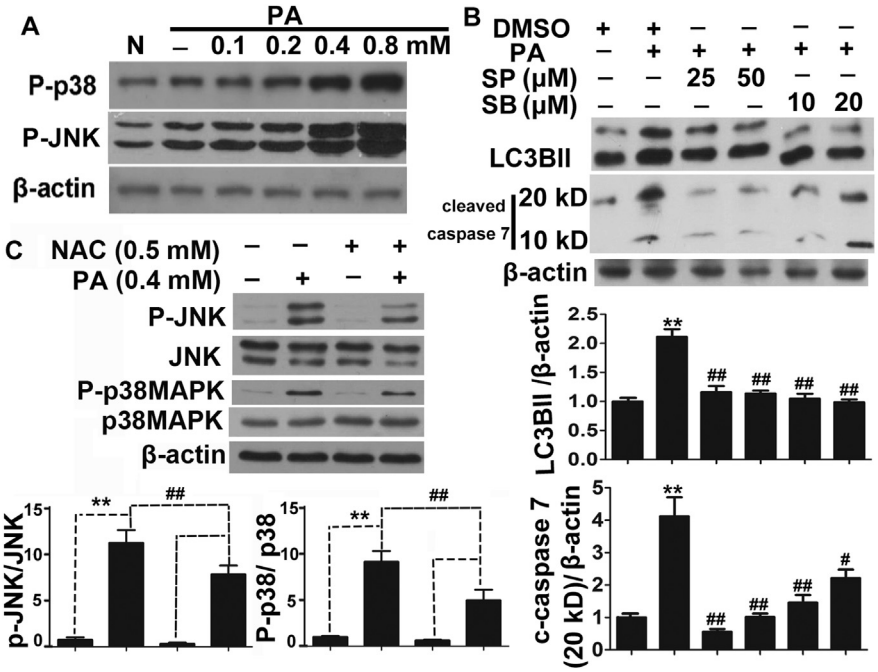

Fig. 4. ROS-dependent activation of JNK and p38 MAPK are involved in inducing apoptosis and autophagy by PA. (A) Western blot analysis of phosphor-JNK, JNK, phosphor-p38 MAPK, p38 MAPK after incubating H9c2 cells with increasing doses of PA (0.1–0.8 mM) for 12 h. Image J software was used to make quantitative analysis of phosphor-JNK/JNK and phosphor-p38 MAPK/p38 MAPK. (B) LC3B II and caspase7 protein levels are determined by Western blot after pretreatment with specific JNK inhibitor SP600125 or p38MAPK inhibitor SB203580 respectively for 1 h followed by 0.4 mM PA for 12 h. (C) H9c2 cells were pretreated with NAC (0.5 mM) followed by 0.4 mM PA for 12 h to detect the effects of ROS on JNK/p38 MAPK signaling. β-actin is probed as loading control. Data represent the mean ± SEM of three independent experiments. $^{**}p < 0.01$, compared with BSA alone-treated group. ##p < 0.01, #p < 0.05, compared with PA alone-treated group.

another study using H9c2 cells as the research object supports our conclusion, which showed that ERK inhibitor reduced PA-induced apoptosis through partial suppression of intracellular ROS generation, suggesting important roles of MAPKs and ROS in H9c2 cells [4]. Thus, we speculate that the effects of PA may be cell type specific and the exact roles of ROS and MAPKs need to be verified *in vivo*.

Overall, this study demonstrates that PA stimulates autophagy and apoptosis via ROS-dependent JNK and p38 MAPK pathways in H9c2 cells. Also, we observed that PA promotes mTORC1-dependent autophagy at an early stage, but blocks autophagic flux for prolonged treatment in H9c2 cells. Although H9c2 cell line may not be an ideal model for primary cardiomyocytes *in vitro*, our findings provide valuable clues to understand the mechanisms of how cardiac cells adapt to PA-induced lipotoxicity.

Conflict of interest

None.

Acknowledgments

This work was supported in part by Chinese National 973 Research Project (No. 2014CB542400), Taishan Scholar Fund and National Natural Science Foundation of China (No. 31070999).

Transparency document

Transparency document related to this article can be found online at http://dx.doi.org/10.1016/j.bbrc.2015.05.042.

References

[1] V.J. Thannickal, B.L. Fanburg, Reactive oxygen species in cell signaling, Am. J. Physiol. Lung Cell. Mol. Physiol. 279 (2000) L1005–L1028.
[2] T. Ozben, Oxidative stress and apoptosis: impact on cancer therapy, J. Pharm. Sci. 96 (2007) 2181–2196.
[3] E.E. Essick, F. Sam, Oxidative stress and autophagy in cardiac disease, neurological disorders, aging and cancer, Oxid. Med. Cell. Longev. 3 (2010) 168–177.
[4] C.D. Wei, Y. Li, H.Y. Zheng, Y.Q. Tong, W. Dai, Palmitate induces H9c2 cell apoptosis by increasing reactive oxygen species generation and activation of the ERK1/2 signaling pathway, Mol. Med. Rep. 7 (2013) 855–861.
[5] H.J. Wang, E.Y. Lee, S.J. Han, S.H. Kim, B.W. Lee, C.W. Ahn, B.S. Cha, H.C. Lee, Dual pathways of p53 mediated glucolipotoxicity-induced apoptosis of rat cardiomyoblast cell: activation of p53 proapoptosis and inhibition of Nrf2-NQO1 antiapoptosis, Metabolism 61 (2012) 496–503.
[6] H. Zhu, Y. Yang, Y. Wang, J. Li, P.W. Schiller, T. Peng, MicroRNA-195 promotes palmitate-induced apoptosis in cardiomyocytes by down-regulating Sirt1, Cardiovasc Res. 92 (2011) 75–84.
[7] J.Y. Kong, S.W. Rabkin, Mitochondrial effects with ceramide-induced cardiac apoptosis are different from those of palmitate, Arch. Biochem. Biophys. 412 (2003) 196–206.
[8] D.L. Hickson-Bick, G.C. Sparagna, L.M. Buja, J.B. McMillin, Palmitate-induced apoptosis in neonatal cardiomyocytes is not dependent on the generation of ROS, Am. J. Physiol. Heart Circ. Physiol. 282 (2002) H656–H664.
[9] M. Park, A. Sabetski, Y. Kwan Chan, S. Turdi, G. Sweeney, Palmitate induces ER stress and autophagy in H9c2 cells: implications for apoptosis and adiponectin resistance, J. Cell. Physiol. 230 (2015) 630–639.
[10] T. Wada, J.M. Penninger, Mitogen-activated protein kinases in apoptosis regulation, Oncogene 23 (2004) 2838–2849.
[11] C.J. Dougherty, L.A. Kubasiak, H. Prentice, P. Andreka, N.H. Bishopric, K.A. Webster, Activation of c-Jun N-terminal kinase promotes survival of cardiac myocytes after oxidative stress, Biochem. J. 362 (2002) 561–571.
[12] A. Porras, S. Zuluaga, E. Black, A. Valladares, A.M. Alvarez, C. Ambrosino, M. Benito, A.R. Nebreda, P38 alpha mitogen-activated protein kinase sensitizes cells to apoptosis induced by different stimuli, Mol. Biol. Cell. 15 (2004) 922–933.
[13] E.J. Park, S.W. Park, H.J. Kim, J.H. Kwak, D.U. Lee, K.C. Chang, Dehydrocostuslactone inhibits LPS-induced inflammation by p38MAPK-dependent induction of hemeoxygenase-1 in vitro and improves survival of mice in CLP-induced sepsis in vivo, Int. Immunopharmacol. 22 (2014) 332–340.
[14] J. Svedberg, P. Bjorntorp, U. Smith, P. Lonnroth, Free-fatty acid inhibition of insulin binding, degradation, and action in isolated rat hepatocytes, Diabetes 39 (1990) 570–574.
[15] A. Matsuzawa, H. Ichijo, Stress-responsive protein kinases in redox-regulated apoptosis signaling, Antioxid. Redox Signal 7 (2005) 472–481.
[16] P.S. Trivedi, L.A. Barouch, Cardiomyocyte apoptosis in animal models of obesity, Curr. Hypertens. Rep. 10 (2008) 454–460.
[17] Z.L. Li, J.R. Woollard, B. Ebrahimi, J.A. Crane, K.L. Jordan, A. Lerman, S.M. Wang, L.O. Lerman, Transition from obesity to metabolic syndrome is associated with altered myocardial autophagy and apoptosis, Arterioscler. Thromb. Vasc. Biol. 32 (2012) 1132–1141.
[18] X. Xu, Y. Hua, S. Nair, Y. Zhang, J. Ren, Akt2 knockout preserves cardiac function in high-fat diet-induced obesity by rescuing cardiac autophagosome maturation, J. Mol. Cell. Biol. 5 (2013) 61–63.
[19] M. Cui, H. Yu, J. Wang, J. Gao, J. Li, Chronic caloric restriction and exercise improve metabolic conditions of dietary-induced obese mice in autophagy correlated manner without involving AMPK, J. Diabetes Res. 2013 (2013) 852754.
[20] S. Lancel, D. Montaigne, X. Marechal, C. Marciniak, S.M. Hassoun, B. Decoster, C. Ballot, C. Blazejewski, D. Corseaux, B. Lescure, R. Motterlini, R. Neviere, Carbon monoxide improves cardiac function and mitochondrial population quality in a mouse model of metabolic syndrome, PLoS One 7 (2012) e41836.
[21] L.E. Gallagher, E.Y. Chan, Early signalling events of autophagy, Essays Biochem. 55 (2013) 1–15.
[22] E.Y. Chan, mTORC1 phosphorylates the ULK1-mAtg13-FIP200 autophagy regulatory complex, Sci. Signal 2 (2009) pe51.
[23] D. Gao, S. Nong, X. Huang, Y. Lu, H. Zhao, Y. Lin, Y. Man, S. Wang, J. Yang, J. Li, The effects of palmitate on hepatic insulin resistance are mediated by NADPH oxidase 3-derived reactive oxygen species through JNK and p38MAPK pathways, J. Biol. Chem. 285 (2010) 29965–29973.
[24] Y. Sato, S. Fujimoto, E. Mukai, H. Sato, Y. Tahara, K. Ogura, G. Yamano, M. Ogura, K. Nagashima, N. Inagaki, Palmitate induces reactive oxygen species production and beta-cell dysfunction by activating nicotinamide adenine dinucleotide phosphate oxidase through Src signaling, J. Diabetes Investig. 5 (2014) 19–26.
[25] J.E. Davis, N.K. Gabler, J. Walker-Daniels, M.E. Spurlock, The c-Jun N-terminal kinase mediates the induction of oxidative stress and insulin resistance by palmitate and toll-like receptor 2 and 4 ligands in 3T3-L1 adipocytes, Horm. Metab. Res. 41 (2009) 523–530.
[26] M. Zhang, C.M. Wang, J. Li, Z.J. Meng, S.N. Wei, J. Li, R. Bucala, Y.L. Li, L. Chen, Berberine protects against palmitate-induced endothelial dysfunction: involvements of upregulation of AMPK and eNOS and downregulation of NOX4, Mediat. Inflamm. 2013 (2013) 260464.
[27] M.S. Han, D.Y. Jung, C. Morel, S.A. Lakhani, J.K. Kim, R.A. Flavell, R.J. Davis, JNK expression by macrophages promotes obesity-induced insulin resistance and inflammation, Science 339 (2013) 218–222.
[28] T.A. Miller, N.K. LeBrasseur, G.M. Cote, M.P. Trucillo, D.R. Pimentel, Y. Ido, N.B. Ruderman, D.B. Sawyer, Oleate prevents palmitate-induced cytotoxic stress in cardiac myocytes, Biochem. Biophys. Res. Commun. 336 (2005) 309–315.